Applied Catalysis B: Environmental 156–157 (2014) 1–7

Contents lists available at ScienceDirect

Applied Catalysis B: Environmental

journal homepage: www.elsevier.com/locate/apcatb

Dimethyl phthalate degradation at novel and efficient electro-Fenton cathode

Yi Wang[a], Yuhui Liu[a], Tianfu Liu[a], Shuqin Song[b], Xuchun Gui[b], Hong Liu[a,c,*], Panagiotis Tsiakaras[d,**]

[a] KLGHEI of Environment and Energy Chemistry/The Key Lab of Low-carbon Chemistry & Energy Conservation of Guangdong Province, School of Chemistry and Chemical Engineering, Sun Yat-sen University, Guangzhou 510275, China
[b] State Key Laboratory of Optoelectronic Materials and Technologies/The Key Lab of Low-carbon Chemistry & Energy Conservation of Guangdong Province, School of Physics and Engineering, Sun Yat-sen University, Guangzhou, China
[c] Chongqing Institute of Green and Intelligent Technology, Chinese Academy of Sciences, Chongqing 401122, China
[d] Department of Mechanical Engineering, School of Engineering, University of Thessaly, Pedion Areos, 38334 Volos, Greece

ARTICLE INFO

Article history:
Received 18 September 2013
Received in revised form 17 February 2014
Accepted 20 February 2014
Available online 28 February 2014

Keywords:
Carbon nanotube sponge
Electro-Fenton
H_2O_2 generation
Dimethyl phthalate

ABSTRACT

A novel three-dimensional porous carbon nanotube sponge (CNTS) with high electrical conductivity was prepared, characterized and investigated as the catalytic cathode for oxygen reduction and employed for an electro-Fenton process to degrade dimethyl phthalate (DMP) in aqueous solution. For comparison, the conventional electro-Fenton cathode, graphite gas diffusion electrode (GDE) and graphite electrode, was also tested. Experiments showed that the side reaction of H_2 evolution was avoided and the H_2O_2 accumulation concentration arrived at the maximal value at CNTS cathode as the cathode potential was set at −0.5 V (*vs.* SCE). The apparent rate constant for DMP degradation was 0.057 min^{-1} at CNTS cathode, much higher than 0.005 min^{-1} at graphite cathode and 0.011 min^{-1} at graphite GDE. Meanwhile, CNTS possessed desirable stability without performance decay after 20 times reaction. It was also found that more negative cathode potential than −0.5 V could cause the side reaction of H_2 evolution and thus leading to a deteriorated DMP degradation. Moreover, the initial DMP concentration affected the apparent rate constant of DMP degradation. Compared to the case of higher initial DMP concentration, DMP degraded faster in the case of lower initial DMP concentration. The pH value and initial Fe^{2+} concentration for DMP degradation at CNTS cathode were optimized to be 3.0 and 0.5 mmol L^{-1}, respectively. The CNTS is promising to be potentially used as the cathode for electro-Fenton system to remove organic pollutants in wastewater.

1. Introduction

Advanced oxidation processes (AOPs) are promising technology for effluent purification when the contaminants are difficult to remove by biological processes [1–4]. Among AOPs, the Fenton oxidation process [5–8], whose high performance is based on the high oxidation power and the non-selective oxidation ability of hydroxyl free radicals (•OH) generated from Fenton's reagents ($H_2O_2 + Fe^{2+}$), has received tremendous attention in recent years. The Fenton's reaction mechanism for the formation of •OH is complicated, while the main reaction can be described as follows:

$$Fe^{2+} + H_2O_2 \rightarrow \bullet OH + OH^- + Fe^{3+} \quad (1)$$

The high oxidative efficiency of Fenton oxidation process has been well established, while its application is limited by the storage and shipment of concentrated hydrogen peroxide (H_2O_2). To solve these problems, electro-Fenton process [9–13] is developed to eliminate or minimize this drawback. In electro-Fenton process, H_2O_2 can be in situ supplied electrochemically through oxygen reduction reaction (ORR), and ferrous ions (Fe^{2+}) can be regenerated at cathode in acidic aqueous solution. Therefore, H_2O_2 production from ORR at cathode is crucial to the electro-Fenton process [14].

It should be noted that ORR has two possible reaction pathways involving two or four electrons transfer, which can be expressed by Eqs. (2) and (3), respectively [15,16].

$$O_2 + 2H^+ + 2e \rightarrow H_2O_2 \quad 0.695\,V \ (vs.\ NHE) \quad (2)$$

* Corresponding author: Tel.: +86 23 63063783; fax: +86 23 84113365.
** Corresponding author: Tel.: +30 24210 74065; fax: +30 24210 74050.
E-mail addresses: liuhong@cigit.ac.cn (H. Liu), tsiak@uth.gr (P. Tsiakaras).

http://dx.doi.org/10.1016/j.apcatb.2014.02.041
0926-3373/

$$O_2 + 4H^+ + 4e \rightarrow 2H_2O \quad 1.229 \ \ V(vs.\ NHE) \qquad (3)$$

Obviously, the 4-electron process of ORR (Eq. (3)) should be avoided as much as possible so that sufficient H_2O_2 can be supplied for the electro-Fenton process. Whether ORR follows two or four-electron process depends strongly on the cathode materials [17,18]. Graphite electrode has been traditionally adopted as the cathode for electro-Fenton system before 2000, because of its high selectivity for 2-electron process of ORR and its low cost. However, due to the limited pore numbers and unsuited pore structure on its surface, their mass transfer characteristics and the electrochemical reaction areas are poor for H_2O_2 generation from ORR. Accordingly, the performance is in need of further improvement for electro-Fenton process, and any effort to identify novel cathode to develop electro-Fenton process should be encouraged [12].

Recently, some novel electro-Fenton cathodes have been investigated, such as carbon gas diffusion electrode (GDE) [12,17,19,20], graphite felt [21], carbon felt [22–24], carbon sponge [25] and so on. In these investigations, the electro-Fenton performance has been enhanced through improving the mass transfer characteristics of cathode. Considering these reports, the novel electro-Fenton electrode materials should possess several characteristics as follows: (1) high selectivity for 2-electron process of ORR, (2) good mass transfer performance, (3) high electrochemical active reaction area, and (4) high electrical conductivity. As reported, carbon nanotubes (CNTs) meet with the above properties. The organic contaminants in wastewater can be quickly destroyed through electro-Fenton process using CNTs electrode as the cathode [26–29].

On the other hand, CNTs generally have a strong tendency to agglomerate due to their nano-size and high surface energy. Therefore, their applications are limited due to the difficulty in dispersing them in a solvent (water or organic agent). Carbon nanotube sponge (CNTS) is a newly developed materials, which is a sponge-like bulk material consisting of self-assembled, interconnected CNT skeletons, a porosity of >99%, high structural flexibility and robustness, high electrical conductivity, and wettability to organics in pristine form [30–32].

Considering that the sponge-like bulk CNTS can be directly used as the cathode for electro-Fenton system, in the present study, CNTS was prepared and directly adopted as the electro-Fenton cathode. Dimethyl phthalate (DMP), widely employed as an indispensable additive of plastics to increase the flexibility, belongs to the family of endocrine disruptor compounds, whose ubiquity in the environment has brought a great concern to academia and public [33,34]. The world annual production of plastics is estimated to be around 100 million tons. DMP has been listed as one of the priority pollutants in some countries including China, and has been used in rapid performance assessment of some AOPs including electro-Fenton reaction [15,33,34]. Herein, it was used as a model substrate to evaluate the cathode performance [33,34,15]. It was found that this electro-Fenton system with CNTS cathode exhibited higher efficiency and desirably recycling stability for degrading DMP.

2. Experimental

2.1. Preparation and characterization of CNTS

CNTS was obtained through a chemical vapor deposition (CVD) process using ferrocene and 1,2-dichlorobenzene as the catalyst precursor and carbon source, respectively. The detailed preparation process has been previously reported [30–32]. In brief, Ferrocene powders were dissolved in dichlorobenzene to obtain a solution (0.06 g mL^{-1}), which was then continuously introduced into a quartz tube fixed in a high-temperature furnace by a syringe pump. The reaction temperature was set at 860 °C. A gas mixture of Ar and H_2, was supplied at a rate of 2000 mL min^{-1} and 300 mL min^{-1}, respectively. A rectangular quartz sheet (2.0 in. × 1.0 in.) was placed in the reaction zone as the growth substrate. After a growth period of 4 h, the sponge-like products were collected from the quartz substrate after CVD. The morphology of the CNTS was obtained by scanning electron microscopy (SEM) (LEO-1530VP, Germany). The X-ray diffraction (XRD) measurements were carried out on a D/Max-IIIA (Rigaku Co., Japan) using Cu Kα radiation (λ = 0.15406 nm), and operating at 40 kV and 40 mA and the scan rate was 10° min^{-1}. Raman spectra were obtained on a Raman spectrometer (Renishaw Corp., UK) using a He/Ne laser with the wavelength of 514.5 nm.

2.2. H_2O_2 generation and DMP degradation

The H_2O_2 generation and DMP degradation experiments were carried out in an undivided glass cell on a Metrohm Autolab PGSTAT302N instrument. The as-prepared CNTS (2.0 cm × 2.0 cm) was used as the cathode (working electrode), a Pt foil and a saturated calomel electrode (SCE) were used as the anode (counter electrode) and the reference electrode, respectively. In the case of H_2O_2 generation, 120 mL of 0.1 mol L^{-1} Na_2SO_4 solution at initial pH 3.0 was used as the electrolyte. In the DMP degradation experiment, Fe^{2+} and DMP with different concentrations were introduced into the above electrolyte. O_2 was fed onto the cathode surface at a flow rate of 400 mL min^{-1}. Without specification, the potentials applied in this study were referred to the SCE.

2.3. Analysis

Linear sweeping voltammetry (LSV) was adopted to investigate and identify the potential for ORR under specific conditions. H_2O_2 concentration was determined by the potassium titaniumoxalate method using a UV–VIS spectrophotometer (TU1810, Universal Analysis, Beijing, China) [33]. The DMP concentration was measured by HPLC (Techcomp, LC 2130, Shanghai, China) equipped with a reverse phase column (Waters, XT erra MS C-18, 5 μm) and a UV detector. The mobile phase was a mixed solution of 50% acetonitrile and 50% water (V/V), and the detection wavelength was set at 276 nm. The total organic carbon (TOC) concentration was determined using a TOC analyzer (Shimadzu 5000A).

3. Results and discussion

3.1. Characteristics of CNTS electrode

As can be clearly seen from Fig. 1A, the as-prepared CNTS appears as a macroscopic and monolithic sponge. The further amplifying observation through SEM (Figs. 1B and C) shows the porous morphology and overlapped carbon nanotubes (CNTs). Moreover, the sponge consists of CNTs self-assembled into a porous, interconnected, and three-dimensional framework. The corresponding diameter and length of multi-walled nanotubes are in the range of 30–50 nm and tens to hundreds of micrometers, indicating that there are multiple layers of CNTs existing in the bulk sponge.

The XRD patterns of the CNTS are shown in Fig. 2A. The characteristic diffraction peaks of graphite carbon at about 26 and 45°, corresponding to (0 0 2) and (1 0 0) face, respectively [35,36]. It indicates a high graphitization and thus a high electrical conductivity with a value of 6×10^{-3} Ω m obtained from a two-probe measurement. This behavior is quite beneficial as the cathode in the electro-Fenton system. The high graphitization can also be confirmed from the Raman spectra of CNTS as given in Fig. 2B. The peak at 1365 cm^{-1} is assigned to the disordered graphite (D-line). The peak at high frequency of 1591 cm^{-1} corresponds to a splitting of the E_{2g} stretching mode of graphite and reflects the structural

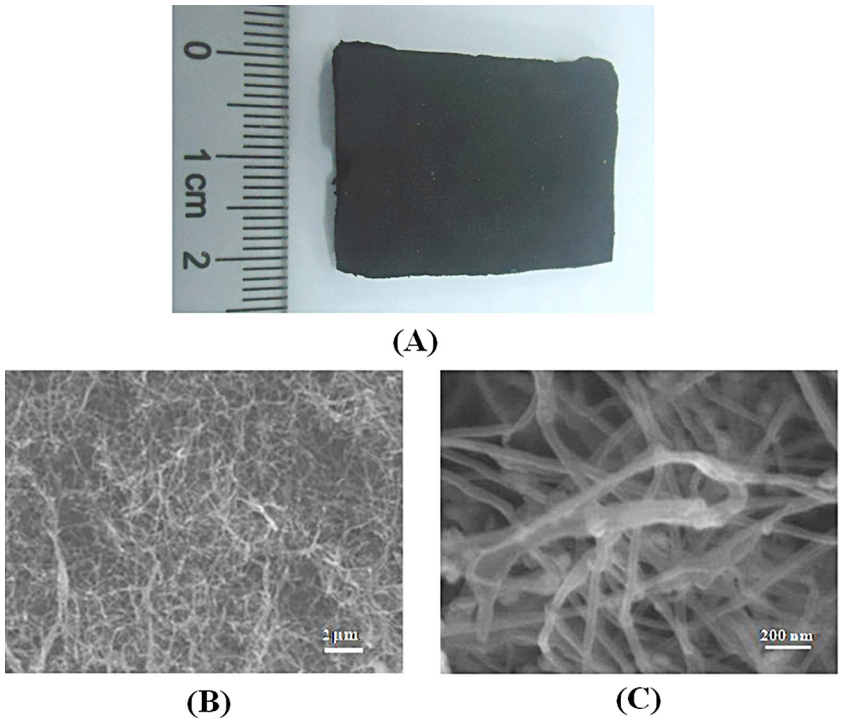

Fig. 1. Macroscopical and microscopic morphology of the as-prepared CNTS: (A) a monolithic sponge and (B and C) cross-sectional SEM image.

intensity of the sp^2-hybridized carbon atom, which denotes for G-line [37]. The intensity ratio between D-line and G-line can be used as an indicator for the extent of graphitization of carbon materials [38]. Based on the Raman curves, it can be calculated that the intensity ratio of D-line to G-line is 0.47, which is much lower than the corresponding value (0.8–1.0) of carbon nanotubes [36,37,39,40]. This further indicates the higher graphitization of CNTS with respect to the carbon nanotubes powders.

3.2. H_2O_2 accumulation concentration at the CNTS electrode

The generation rate of H_2O_2 plays an important role in the DMP degradation by electro-Fenton technology. Considering that the constant potential mode is usually used to derive fundamental electrochemical information in lab-scale experiments, a constant cathode potential was adopted for the H_2O_2 generation and for the electro-Fenton system in the present investigation. Consequently, the determination of the applied potential range is quite important to guarantee the effective H_2O_2 generation through ORR via 2-electron process. For this purpose, LSV curves were initially obtained for CNTS cathode in the presence of saturated O_2 or N_2 at a scan rate of 10 mV s^{-1} and the results are shown in Fig. 3. In the case of pure N_2, the only reaction of H_2 evolution exists, which starts from ca. −0.60 V. In the case of saturated O_2, since 0 V, ORR starts and the corresponding current increases until a small plateau appears in the range of about −0.50 and −0.70 V. After that the current increases rapidly, which could be due to that H_2 evolution sharply occurs. Consequently, in order to avoid H_2 evolution reaction, it is not difficult to infer that the potential from −0.5 and −0.6 V is suitable range for H_2O_2 generation through ORR at CNTS cathode.

The H_2O_2 accumulation was then investigated at different applied cathode potentials and the results are presented in Fig. 4. It can be distinguished that at CNTS cathode, H_2O_2 concentration arrives at the maximal value (24 mg L^{-1}) when the cathode potential is set at −0.5 V. This result agrees well with the LSV results (Fig. 3). In one of Zhou's works [41], the operating conditions were as follows: pH = 3, $[Na_2SO_4]$ = 0.1 mol L^{-1}, V = 0.2 L, O_2 flow rate = 500 mL min^{-1}, and cathode potential = −0.72 V, graphite-felt (Carbone Loraine, 15 cm × 4 cm). Their H_2O_2 accumulation concentration in 60 min was ~40 mg L^{-1}. While, in our present case, the operation conditions as given above were pH = 3, $[Na_2SO_4]$ = 0.1 mol L^{-1}, V = 0.1 L, O_2 flow rate = 400 mL min^{-1}, and cathode potential = −0.5 V, CNTS (2.0 cm × 2.0 cm). Under these conditions, the H_2O_2 accumulation concentration in 60 min was ~24 mg L^{-1}. So, if we compared the H_2O_2 accumulation concentration per min per electrode area, our case is better. However, due to the fact that there is no the same comparison basis, the comparison seems unreasonable. From −0.3 to −0.5 V, the current for ORR to generate H_2O_2 increases and thus leads to the enhanced H_2O_2 yield. From −0.7 to −1.1 V, the H_2 evolution as a side reaction occurs and restrains the ORR to generate H_2O_2. Consequently the H_2O_2 yield is reduced as the applied cathode potential increases.

3.3. The electro-Fenton degradation of DMP

3.3.1. DMP degradation: CNTS vs. graphite electrode and graphite GDE

In order to confirm the effectiveness of CNTS, the conventional electro-Fenton cathode, graphite electrode and graphite gas diffusion electrode (GDE), with the same geometric surface area was adopted as comparison for DMP degradation. As demonstrated in Fig. 5A, CNTS have a significantly higher DMP degradation efficiency, with 96% on CNTS versus 26% on graphite electrode and 48% on graphite GDE after 60 min. As shown in the inset of Fig. 5B, the corresponding degradation rate constants are 0.005, 0.011 and 0.057 min^{-1} at graphite, graphite GDE, and CNTS cathode, respectively. The mineralization of DMP was also investigated and it was found that CNTS cathode could remove 75% TOC in 2 h, while only 10% and 35% TOC removal was obtained at graphite electrode and graphite GDE, respectively. This could be attributed to the easier O_2 mass transfer and bigger electrochemical active area from the suitable porous structure of CNTS, which is beneficial for H_2O_2 generation from ORR and then DMP degradation. Consequently,

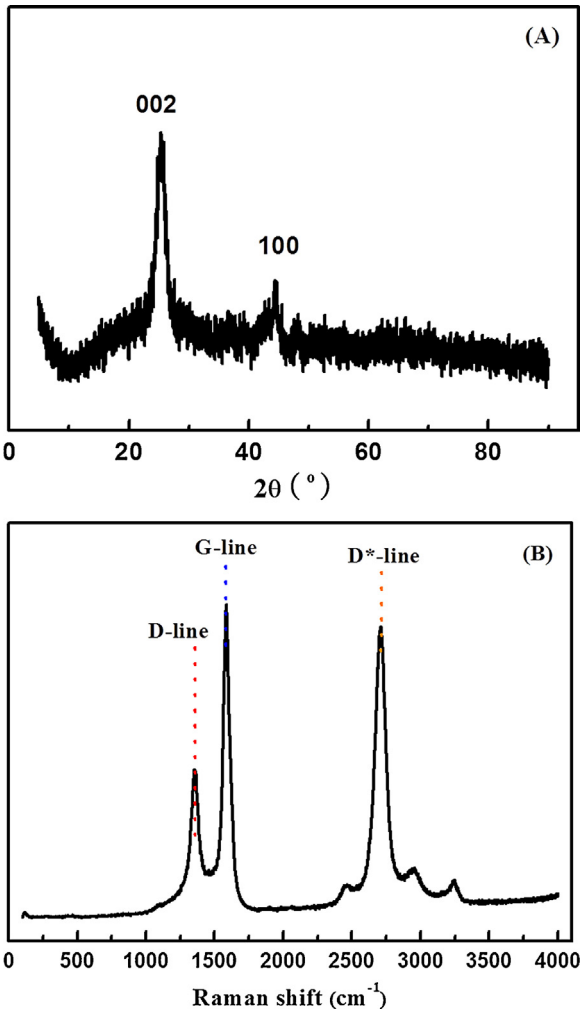

Fig. 2. The XRD pattern (A) and Raman spectra (B) of the as-prepared CNTS.

it implies that CNTS can be employed as an effective cathode for electro-Fenton technology.

3.3.2. Comparison of adsorption, oxidation by oxygen and electro-Fenton process

In the electro-Fenton process for DMP degradation at CNTS cathode, the DMP adsorption by CNTS and its direct oxidation by O_2 likewise leads to the decrease in the DMP concentration. To investigate the DMP removal efficiency only through the electro-Fenton process, the DMP removal efficiency by the adsorption or oxidation by O_2 were carried out. Fig. 6 presents the DMP removal efficiencies along with time using only adsorption, oxidation by O_2 and the electro-Fenton technology. It can be clearly seen that there is only a slight difference between the DMP removal efficiencies by pure adsorption and oxidation by O_2. And in both cases DMP removal

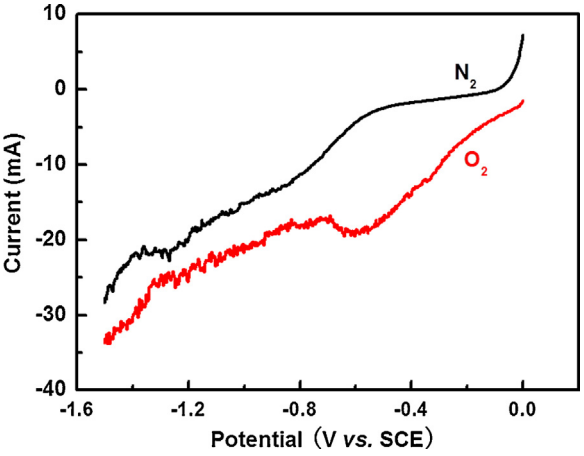

Fig. 3. The linear sweeping voltammetric curves for CNTS cathode in 0.1 mol L^{-1} Na_2SO_4 solution (pH = 3.0) in the presence of saturated O_2 or N_2. Sweeping rate: 10 mV s^{-1}.

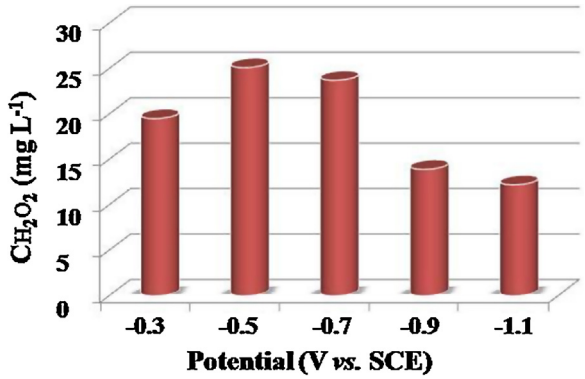

Fig. 4. The H_2O_2 yields using CNTS as electro-Fenton cathode with different applied cathode potentials. The electrolyte was 0.1 mol L^{-1} Na_2SO_4 and the solution pH value was 3.0.

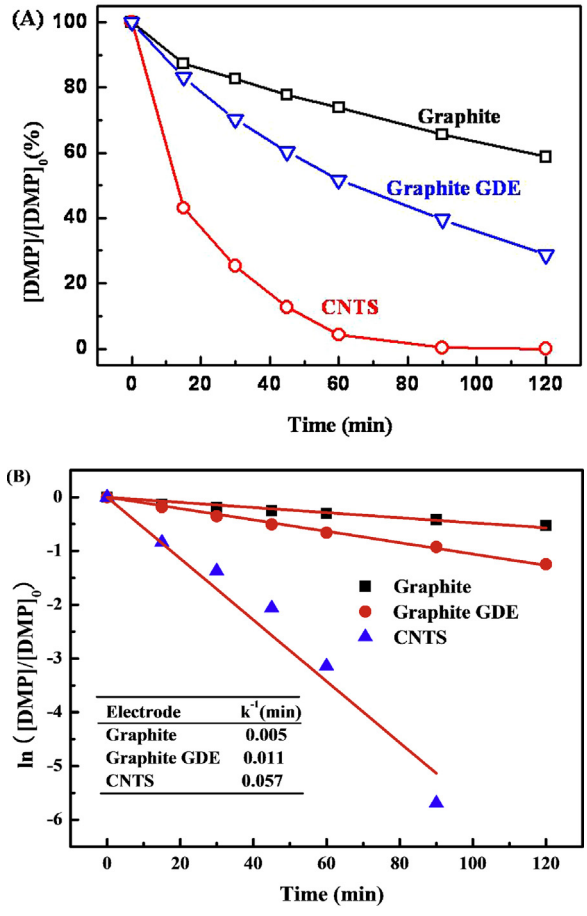

Fig. 5. (A) DMP degradation efficiency as a function of time at CNTS and graphite and graphite GDE cathodes, initial pH = 3.0, $[Fe^{2+}]$ = 0.5 mmol L^{-1}, and (B) the corresponding DMP degradation kinetics at CNTS and graphite and graphite GDE cathodes.

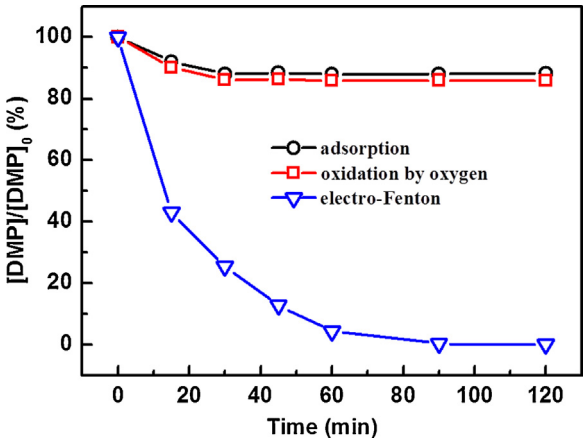

Fig. 6. Variation of DMP removal efficiency with time at pH 3.0. For adsorption: no oxygen was supplied and the current was turned off. For oxygen oxidation: oxygen supplying rate: 400 mL min^{-1}. For electro-Fenton: applied cathode potential: −0.5 V.

efficiency falls in 11–13% after 120 min. Clearly, either adsorption or oxidation by O_2 is not an effective way to remove DMP. By contrast, the electro-Fenton technology has a much higher DMP removal efficiency, and DMP can be almost completely removed in only 60 min. It is easily inferred that most of DMP removal was achieved by the electro-Fenton process.

3.3.3. *Effect of applied cathode potential on electro-Fenton process*

In order to identify the suitable applied cathode potential for optimal and effective DMP removal, a set of experiments with different cathode potentials were carried out and the corresponding results are shown in Fig. 7. It can be clearly seen from Fig. 7A that the respective [DMP]/[DMP]$_0$ in 60 min are 11.4%, 4.3%, 4.6%, 19.6% and 25.4% for −0.3, 0.5, −0.7, −0.9 and −1.1 V. It was found that the concentration–time curves for the DMP degradation were well fitted by the kinetic model of pseudo-first-order reaction below:

$$\mathrm{Ln}\frac{[\mathrm{DMP}]}{[\mathrm{DMP}]_0} = -kt \quad (6)$$

where [DMP]$_0$ and [DMP] are the initial DMP concentration and the DMP concentration at time t, respectively, and k is the apparent rate constant. The results of Ln([DMP]/[DMP]$_0$) against t are shown in Fig. 7B. The DMP degradation shows that the maximal apparent rate constant (k) arrives at 0.057 min^{-1} at the cathode potential of −0.5 V as seen from the inset of Fig. 7B. So, the optimized applied cathode potential at CNTS electrode is −0.5 V. At −0.3 V, both DMP removal efficiency and k value are less than those at −0.5 V. This could be due to the lower generation rate of H_2O_2 and then the reduced concentration of hydroxyl free radicals. In the case of cathode potential less than −0.5 V, the DMP removal efficiency and k value decreases as the cathode potential increases. This is due to that the decreased potential triggers the occurrence of H_2 evolution reaction, and in this way leads to the reduced H_2O_2 yield as above discussed in Figs. 3 and 4 and consequently a lower DMP removal efficiency.

3.3.4. *Effect of initial DMP concentration*

Fig. 8 shows DMP degradation kinetics at different initial DMP concentrations. The detailed values are summarized in Table 1. It is obvious that the DMP removal efficiency varies with its initial concentration. At lower concentration, 20 mg L^{-1}, DMP removal is very fast, with 100% DMP removal efficiency after 30 min reaction. Furthermore, along with the increment of DMP concentration, DMP removal efficiency decreases significantly, from 95.7% at 50 mg L^{-1} to 66.1% at 100 mg L^{-1} and 45.4% at 150 mg L^{-1} in 60 min. From

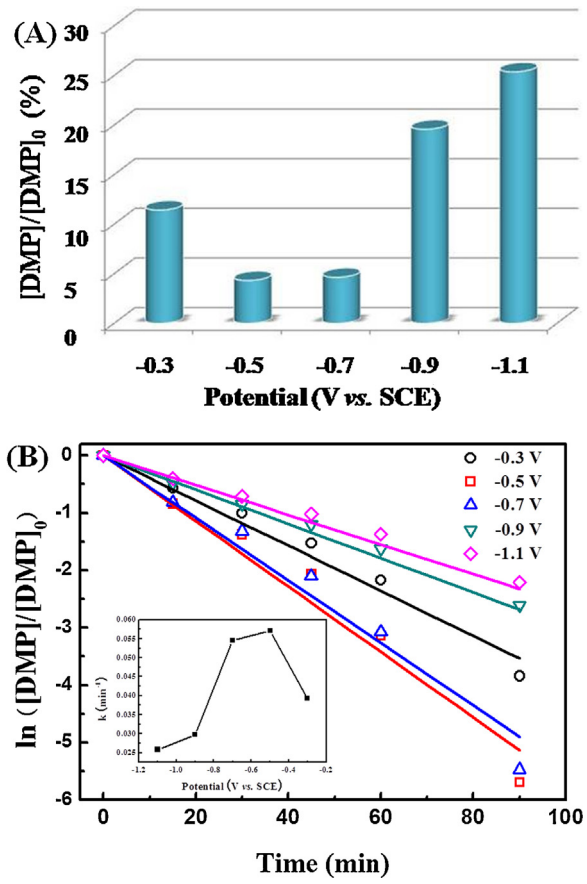

Fig. 7. Effect of the applied cathode potential on the DMP degradation efficiency (A) and kinetics of the DMP degradation (B), initial pH = 3.0, and [Fe^{2+}] = 0.5 mmol L^{-1}.

Fig. 8, it can also be seen that DMP degradation follows the pseudo first-order reaction kinetics with the different rate constants at varying initial DMP concentration. As also seen from Table 1, the apparent rate constant of DMP decreases as the initial DMP concentration increases, which may be due to the availability of constant amount of hydroxyl radicals irrespective of the DMP concentration. The bigger initial DMP concentration could lead to the higher concentration of by-products of DMP oxidation, which will react with hydroxyl radicals, thus leading to slower decay kinetics [42,43].

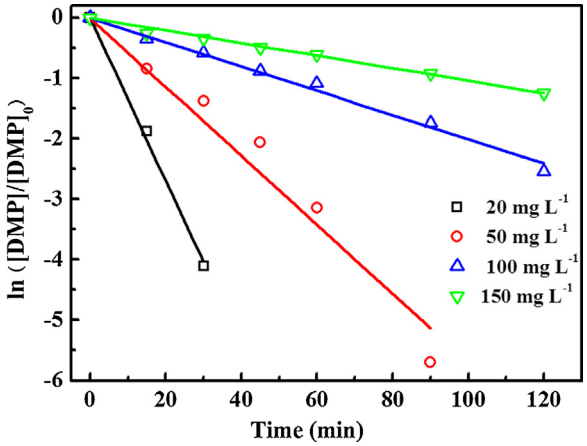

Fig. 8. DMP degradation kinetics at different initial DMP concentrations, initial pH = 3.0, and [Fe^{2+}] = 0.5 mmol L^{-1}.

Table 1
The apparent rate constants of DMP degradation with varying initial DMP concentration and the residual DMP percentage in 60 min reaction, pH = 3.0, and $[Fe^{2+}] = 0.5\ mmol\ L^{-1}$.

Initial DMP concentration ($mg\ L^{-1}$)	Apparent rate constant (min^{-1})	Residual DMP (%) in 60 min
20	0.134	0.0[a]
50	0.057	4.3
100	0.020	33.9
150	0.010	54.6

[a] In the case of 20 $mg\ L^{-1}$ of initial DMP concentration, DMP was completely degraded in 30 min reaction.

3.3.5. Effect of solution pH value

The solution pH value commonly has a significant effect on the electro-Fenton process. From Eq. (2), it can be known that a high concentration H^+ (a low pH value) is helpful for H_2O_2 production. On the other hand, based on Eq. (4), it can also be known that a low pH value also leads to the side reaction of H_2 evolution. This inevitably takes up at least some active sites for H_2O_2 production. At the same time, according to Eq. (5), the pH value should be less than 6.6 in order to avoid the formation of $Fe(OH)_2$ precipitation in the case of 0.5 $mmol\ L^{-1}$ Fe^{2+} in the solution.

$$2H^+ + 2e^- \rightarrow H_2 \quad 0\ V \ (vs.\ \ NHE) \tag{4}$$

$$Fe^{2+} + 2OH^- = Fe(OH)_2 \downarrow \quad K_{sp} = 8.0 \times 10^{-16} \tag{5}$$

Meanwhile, at low pH value, $Fe(OH)^+$ could be formed, which will compete with Fe^{2+} to react with H_2O_2. However, $Fe(OH)^+$ reacts more slowly with H_2O_2 and thus leads to less hydroxyl radicals. Moreover, at very low pH value, hydroxyl radicals will be scavenged by H^+ and the reaction between Fe^{2+} and H_2O_2 is inhibited [44–46].

Consequently, there should exist an optimal solution pH value for the electro-Fenton process for DMP degradation at CNTS electrode. The effect of the initial pH value on the DMP degradation kinetics is given in Fig. 9. The apparent rate constants are 0.050, 0.057, and 0.02 min^{-1} for pH value 1.0, 3.0, and 5.0, respectively. So, the optimal pH value was 3.0 for DMP degradation at CNTS electrode.

3.3.6. Effect of initial Fe^{2+} concentration

A set of experiments were carried out to investigate the effect of the initial Fe^{2+} concentration on DMP degradation kinetics and the results are shown in Fig. 10. It can be clearly seen from Fig. 10 that the apparent rate constants of DMP degradation increase from 0.016 to 0.057 min^{-1} along with Fe^{2+} concentration changing from 0.2 to 0.5 $mmol\ L^{-1}$. This is because the quantity of generated •OH is directly dependent on the Fe^{2+} dosage according to Eq. (1). Whereas, in the case of the further increase of Fe^{2+} to 1.0 $mmol\ L^{-1}$, the apparent rate constant of DMP degradation decreases to 0.045 min^{-1}. This could be resulted from the reaction of Fe^{2+} and •OH (Eq. (6)), which is several orders of magnitude faster than Eq. (1) for •OH generation:

$$Fe^{2+} + \bullet OH \rightarrow Fe^{3+} + OH^- \tag{6}$$

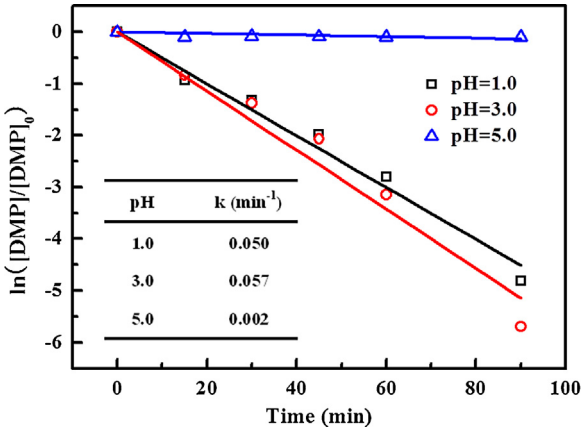

Fig. 9. DMP degradation kinetics at different initial pH values, initial DMP concentration: 50 $mg\ L^{-1}$, and $[Fe^{2+}] = 0.5\ mmol\ L^{-1}$.

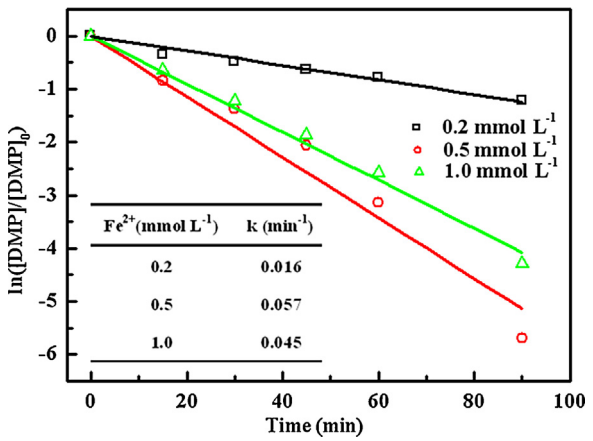

Fig. 10. DMP degradation kinetics at different initial Fe^{2+} concentrations, initial DMP concentration: 50 $mg\ L^{-1}$, and initial pH = 3.0.

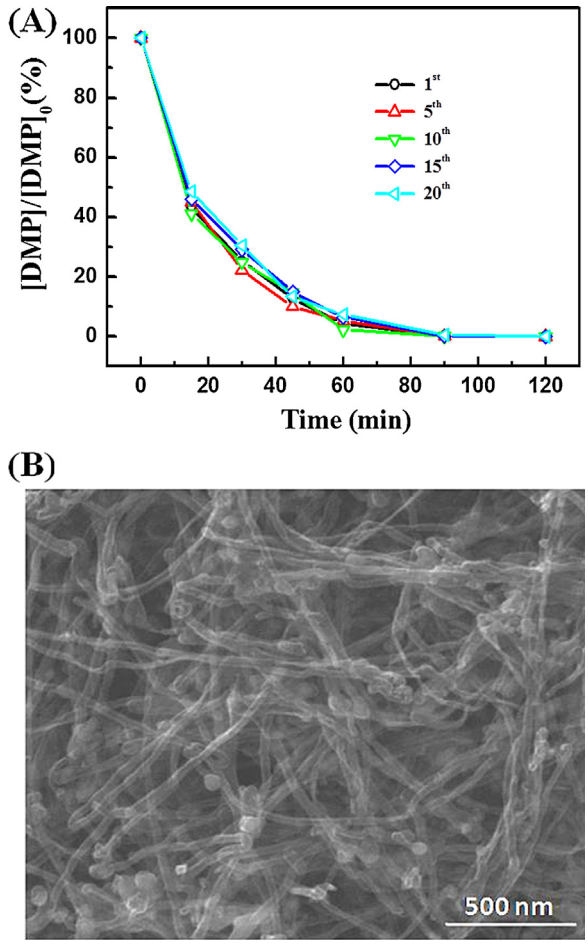

Fig. 11. The recycling experiments of the DMP degradation by electro-Fenton reaction using different cathodes potential in 120 min, initial pH = 3.0, $[Fe^{2+}] = 0.5\ mmol\ L^{-1}$, and initial DMP concentration: 50 $mg\ L^{-1}$.

Furthermore, the produced Fe^{3+} could react with H_2O_2 to produce hydroperoxyl radicals (HO_2•) but not hydroxyl radicals (Eqs. (7) and (8)) [42]. Considering that the oxidation capability of hydroperoxyl is much less than that of hydroxyl radicals, the DMP degradation consequently decreased.

$$Fe^{3+} + H_2O_2 \rightarrow Fe - OOH^{2+} + H^+ \quad (7)$$

$$Fe{-}OOH^{2+} \rightarrow HO_2\bullet + Fe^{2+} \quad (8)$$

Consequently, •OH concentration was reduced and thus the DMP degradation kinetics was decreased. Based on the experimental results, the initial Fe^{2+} concentration was optimized to be 0.5 mmol L^{-1}.

3.3.7. Long-term performance for DMP degradation

The long-term performance of CNTS electrode for DMP degradation was further investigated. Fig. 11A shows the effect of the reuse of CNTS electrode on DMP degradation at −0.5 V. There is no obvious difference after 20 times reactions with a 120-min reaction time each. Moreover, DMP can be almost completely and quickly degraded. It should be also noted that there is no obvious damage for the bulk CNTS electrode from the naked eyes after these long-term performance investigations. The further SEM image (Fig. 11B) confirms CNTS keeps its initial porous interconnected microscopic structure. This implies that the stability of CNTS can be maintained for a long time and it can be reused. This could be benefited from the intrinsic stability of chemical and physical properties of carbon nanotubes, as well as the interconnected and three-dimensional overlapped framework of CNTS obtained through the self-assemble of carbon nanotubes.

4. Conclusions

A novel three-dimensional CNTS was synthesized and used to degrade DMP in an aqueous solution as the cathode of an electro-Fenton process. The CNTS with the structure of a macroscopic and monolithic sponge consists of CNTs self-assembled into a porous, interconnected, and three-dimensional framework. Moreover, the CNTS possesses high electrical conductivity with a value of 6×10^{-3} Ω m due to the high graphitization. Adopting CNTS as the cathode in electro-Fenton system, the side reaction of H_2 evolution was avoided and H_2O_2 concentration arrived at the maximal value when the applied cathode potential was −0.5 V. The DMP degradation experiments showed that at CNTS cathode, the apparent rate constant for DMP degradation was 0.057 min^{-1}, ten times higher than that (0.005 min^{-1}) at graphite cathode. Meanwhile, CNTS showed a desirable stability without performance decay after 20 times reaction. It was also found that DMP degradation followed the pseudo first-order reaction kinetic at CNTS cathode. The biggest apparent rate constant for DMP degradation was obtained at −0.5 V at CNTS cathode and DMP degradation apparent rate constant decreased as the initial DMP concentration increased. The optimal pH value and initial Fe^{2+} concentration for DMP degradation at CNTS cathode were 3.0 and 0.5 mmol L^{-1}, respectively. The CNTS is an attractive alternative cathode for electro-Fenton system to the degradation of organic contaminants in wastewater.

Acknowledgements

This work was supported by the Natural Science Foundation of China (21107145, 51378494 and 21077136), the project of Pearl River Science and Technology New Star of Guangzhou (2011Z220061), the Fundamental Research Funds for the Central Universities of China (12gpy13), and the Key Project of Science and Technology of Guangdong Province (No. 2010B01090033).

References

[1] S. Cao, K.L. Yeung, J.K.C. Kwan, P.M.T. To, S.C.T. Yu, Appl. Catal. B: Environ. 3–4 (2009) 127–136.
[2] W.R. Chen, C.M. Sharpless, K.G. Linden, I.H. Suffet, Environ. Sci. Technol. 40 (2006) 2734–2739.
[3] T. Yamamoto, S.I. Kim, J. Chaichanawong, E. Apiluck, T. Ohmori, Appl. Catal. B: Environ. 3–4 (2009) 455–461.
[4] N. Sano, T. Yamamoto, I. Takemori, S. Kim, A. Eiad-ua, D. Yamamoto, M. Nakaiwa, Ind. Eng. Chem. Res. 45 (2006) 2897–2900.
[5] C.K. Duesterberg, S.E. Mylon, T.D. Waite, Environ. Sci. Technol. 42 (2008) 8522–8527.
[6] C.K. Duesterberg, T.D. Waite, Environ. Sci. Technol. 40 (2006) 4189–4195.
[7] S. Navalon, A. Dhakshinamoorthy, M. Alvaro, H. Garcia, ChemSusChem 4 (2011) 1712–1730.
[8] J.J. Pignatello, E. Oliveros, A. MacKay, Crit. Rev. Environ. Sci. Technol. 36 (2006) 1–84.
[9] E. Brillas, E. Mur, R. Sauleda, L. Sánchez, J. Peral, X. Domènech, J. Casado, Appl. Catal. B: Environ. 16 (1998) 31–42.
[10] E. Brillas, J.C. Calpe, J. Casado, Water Res. 34 (2000) 2252–2262.
[11] C.A. Martínez-Huitle, E. Brillas, Appl. Catal. B: Environ. 87 (2009) 105–145.
[12] E. Brillas, I. Sirés, M.A. Oturan, Chem. Rev. 109 (2009) 6570–6631.
[13] M.A. Oturan, J. Appl. Electrochem. 30 (2000) 475–482.
[14] R. Emilio, P.M. Sanroman, M. Angeles, Chem. Eng. Technol. 35 (2012) 609–617.
[15] H. Liu, C. Wang, X. Li, X. Xuan, C. Jiang, H. Cui, Environ. Sci. Technol. 41 (2007) 2937–2942.
[16] H. Liu, X. Li, Y. Leng, C. Wang, Water Res. 41 (2007) 1161–1167.
[17] C.T. Wang, J.L. Hu, W.L. Chou, Y.M. Kuo, J. Hazard. Mater. 152 (2008) 601–606.
[18] M.H.M.T. Assumpc, R.F.B. De Souza, D.C. Rascio, J.C.M. Silva, M.L. Calegaro, I. Gaubeur, T.R.L.C. Paixão, P. Hammer, M.R.V. Lanza, M.C. Santos, Carbon 49 (2011) 2842–2851.
[19] L.C. Almeida, S. Garcia-Segura, C. Arias, N. Bocchi, E. Brillas, Chemosphere 89 (2012) 751–758.
[20] Z.X. Wang, G. Li, F. Yang, Carbohydr. Polym. 86 (2011) 1807–1813.
[21] M. Panizza, M.A. Oturan, Electrochim. Acta 56 (2011) 7084–7087.
[22] A.M. Wang, Y.Y. Li, A.L. Estrada, Appl. Catal. B: Environ. 102 (2011) 378–386.
[23] N. Oturan, M. Hamza, S. Ammar, J. Electroanal. Chem. 661 (2011) 66–71.
[24] C.T. Wang, W.L. Chou, M.H. Chung, Y.M. Kuo, Desalination 253 (2010) 129–134.
[25] A. Özcan, Y. Şahin, A.S. Koparal, M.A. Oturan, J. Electroanal. Chem. 616 (2008) 71–78.
[26] A.R. Khataee, M. Zarei, Desalination 278 (2011) 117–125.
[27] M. Zarei, A. Niaei, D. Salari, A.R. Khataee, J. Electroanal. Chem. 639 (2010) 167–174.
[28] X.W. Zhang, L.C. Lei, B. Xia, Y. Zhang, J.L. Fu, Electrochim. Acta 54 (2009) 2810–2817.
[29] A.R. Khataee, M. Safarpour, M. Zarei, J. Mol. Catal. A: Chem. 363 (2012) 58–68.
[30] X.C. Gui, J.Q. Wei, K.L. Wang, A.Y. Cao, H.W. Zhu, Y. Jia, Q.K. Shu, D.H. Wu, Adv. Mater. 22 (2010) 617–621.
[31] X.C. Gui, A.Y. Cao, J.Q. Wei, H.B. Li, Y. Jia, Z. Li, L.L. Fan, K.L. Wang, H.W. Zhu, D.H. Wu, ACS Nano 4 (2010) 2320–2326.
[32] H.B. Li, X.C. Gui, L.H. Zhang, C.Y. Ji, Y.C. Zhang, P.Z. Sun, J.Q. Wei, K.L. Wang, H.W. Zhu, D.H. Wu, A.Y. Cao, Adv. Funct. Mater. 221 (2011) 3439–3445.
[33] B.L. Yuan, X.Z. Li, N. Graham, Water Res. 42 (2008) 1413–1420.
[34] B.L. Yuan, X.Z. Li, N. Graham, Chemosphere 72 (2008) 197–204.
[35] D. Liang, J. Gao, H. Sun, P. Chen, Z.Y. Hou, X.M. Zheng, Appl. Catal. B: Environ. 3–4 (2011) 423–432.
[36] C.M. Chen, Y.M. Dai, J.G. Huang, J.M. Jehng, Carbon 44 (2006) 1808–1820.
[37] C. He, S. Song, J. Liu, V. Maragou, P. Tsiakaras, J. Power Sources 195 (2010) 7409–7414.
[38] R. Nie, J. Wang, L. Wang, Y. Qin, P. Chen, Z. Hou, Carbon 50 (2012) 586–596.
[39] D. Liang, J. Gao, H. Sun, P. Chen, Z. Hou, X. Zheng, Appl. Catal. B: Environ. 106 (2011) 423–432.
[40] J. Zhang, H.L. Zou, Q. Qing, Y.L. Yang, Q.W. Li, Z.F. Liu, X.Y. Guo, Z.L. Du, J. Phys. Chem. B 107 (2003) 3712–3718.
[41] M. Zhou, Q. Tan, Q. Wang, Y. Jiao, N. Oturan, M.A. Oturan, J. Hazard. Mater. 215–216 (2012) 287–293.
[42] F. Almomani, E.A. Baranova, Environ. Technol. 34 (2013) 1473–1479.
[43] A. Babuponnusamia, K. Muthukumarb, Chem. Eng. J. 183 (2012) 1–9.
[44] J.J. Pignatello, Environ. Sci. Technol. 26 (1992) 944–951.
[45] N. Masomboon, C. Ratanatamskul, M.C. Lu, J. Hazard. Mater. 176 (2010) 92–98.
[46] Y.R. Wang, W. Chu, Water Res. 45 (2011) 3883–3889.